A&A 427, 755–761 (2004)
DOI: 10.1051/0004-6361:20047131


Astronomy & Astrophysics

# The phase curve of cometary dust: Observations of comet 96P/Machholz 1 at large phase angle with the SOHO LASCO C3 coronagraph

Ye. Grynko, K. Jockers, and R. Schwenn

Max-Planck-Institut für Sonnensystemforschung⋆, Max-Planck-Strasse 2, 37191 Katlenburg-Lindau, Germany
e-mail: grynko@linmpi.mpg.de

Received 23 January 2004 / Accepted 20 July 2004

**Abstract.** We have analyzed brightness and polarization data of comet 96P/Machholz, obtained with the SOHO-LASCO C3 coronagraph at phase angles up to 167° and 157°, respectively. The polarization data are characteristic of a typical dusty comet. Within error limits the corresponding trigonometric fit describes the new data measured at larger phase angles as well as those of the previously known range. In the phase angle range from 110° to 167° the brightness increases almost linearly by about two orders of magnitude. The gradient is independent of wavelength. From the absence of a diffraction spike we conclude that the grains contributing significantly to the scattered light must have a size parameter $x = 2\pi r/\lambda \geq 20$, i.e. have a radius larger than 1 $\mu$m. Fits of the data with Mie calculations of particles having a power law distribution of power index $\approx 2.5$ provide a best fit refractive index $m = 1.2 + i0.004$. In the framework of effective medium theory and on the assumption of a particle porosity $P = 0.5$ this leads to a complex refractive index of the porous medium $m = 1.43 + i0.009$. A higher refractive index is possible for more porous grains with very low absorption. The large particle sizes are in qualitative agreement with findings derived from the analysis of the motion of cometary dust under solar radiation pressure (Fulle and coworkers, see Fulle et al. 2000; Jockers 1997) and with the in-situ measurements of the dust of Halley's comet.

**Key words.** comets: individual: 96P/Machholz 1 – techniques: photometric – techniques: polarimetric

## 1. Introduction

Light scattering models of cometary dust suffer from the fact that measurements of brightness and polarization of the scattered light at large phase angles (forward scattering) are almost nonexistent. If a comet is seen from the Earth at large phase angles, most often its solar elongation is very small and observations are impossible. Up to now the largest phase angle at which the brightness of a comet was measured was equal to 149° (comet C/1980 Y1 (Bradfield) = 1980 XV (Gehrz & Ney 1992). For polarization the maximum angle is still smaller. For comets C/1989 X1 (Austin) = 1990 V and C/1996 B2 (Hyakutake) (Kiselev & Velichko 1998) the degree of polarization was measured at =111°. Polarization data of comet C/1999 S4 exist at a maximum phase angle of 121° (Kiselev et al. 1998, Hadamcik & Levasseur-Regourd 2003), but these data were obtained during the disruption of the nucleus and therefore may not be representative. In January 2002 Comet 96P/Machholz 1 was photographed with the C3 coronagraph on board SOHO. On the images suitable for measurements the maximum phase angle is equal to 157° for polarization and 167° for brightness. In this paper we make an attempt to derive brightness and polarization of Comet 96P/ Machholz 1 from the SOHO C3 coronagraph observations.

⋆ Until June 30, 2004 Max-Planck-Institut für Aeronomie.

## 2. Observations

### 2.1. The SOHO spacecraft and LASCO C3 telescope

The Large Angle and Spectrometric Coronagraph (LASCO) instrument is one of 11 instruments operating on the joint ESA/NASA SOHO (Solar and Heliospheric Observatory) spacecraft. The spacecraft was launched in 1995 and was placed in an orbit about the first Lagrangian, or L1, libration point, on the Earth-Sun line where the gravitational attraction of the spacecraft to the Earth is just balanced by its attraction to the Sun.

The three coronagraphs comprising LASCO are designated C1, C2 and C3. C1 covers a field from 1.1 to 3.0 $R_\odot$ (solar radii from Sun center), C3 spans the outer corona from about 3.7 to 32 $R_\odot$, and C2 extends from 2.0 to 6.0 $R_\odot$, i.e. overlaps with both C1 and C3. In this work we have used only C3 data as the comet did not enter the field of view of the other instruments.

C3 has a coronagraph aperture of 9.6 mm diameter, an effective focal length of 77.6 mm and an effective $f$-number $f/9.3$ (Brueckner et al. 1995). Its optical design takes into account the necessity for blocking direct sunlight and obtaining

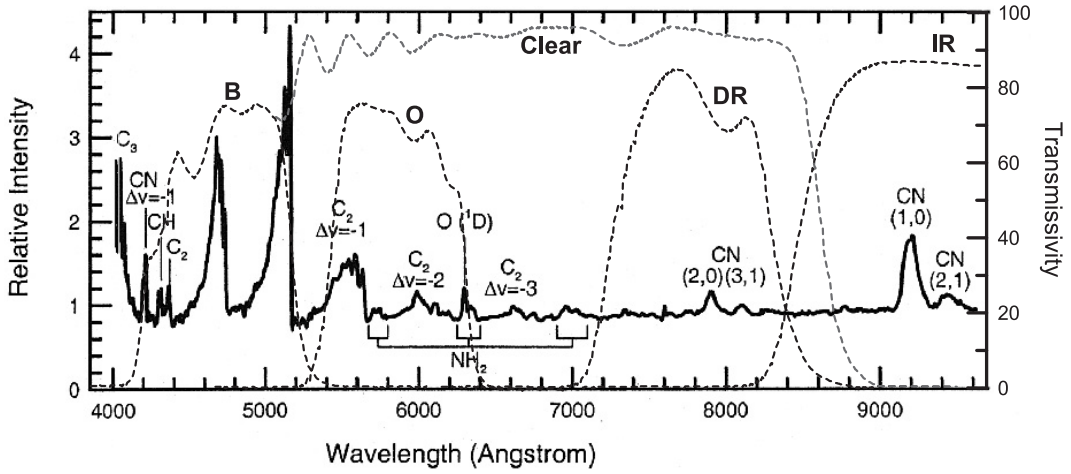


**Fig. 1.** LASCO C3 color filter data (dashed lines) and a cometary spectrum (solid line). Spectrum of comet 109P/Swift-Tuttle curtesy A. Cochran, Univ. of Texas.

absolutely minimal scattering. The filter and polarizer wheels are installed in front of the 21.5 mm square $1024 \times 1024$ pixel CCD detector. The 21 $\mu$m CCD pixel size subtends an angle of 56 arcsec. The CCD square accommodates a 30 $R_\odot$ radius image, so that portions of the 32 $R_\odot$ optical field of view are lost off the top, bottom, left, and right edges of the CCD surface. The image becomes unvignetted beyond 10 $R_\odot$.

C3 was not designed for narrowband observations and therefore does not have narrowband, spectroscopic quality filters. It has broadband color filters for the purpose of separation of the F from the K corona and polarizers for polarization analysis. The filter wheel contains the blue, orange, deep red, and infrared filters, and a clear glass position. Their bandwidths are indicated in Fig. 1. The polarizer wheel contains three polarizers at 120 degrees (their positions are designated as "−60°","0°", and "+60°"), the H-alpha filter, and a clear glass position. The SOHO mission was interrupted in June 1998, and due to excessive cold the "0°" polarizing filter was damaged. After that the only thing we could do was to use the clear filter to calculate a synthetic "0°" image, according to the technique applied in the polarization routines of the LASCO IDL software library.

### 2.2. Available SOHO data and the orbit of Comet 96P/Machholz 1

Between January 5 and 10, 2002, comet 96P/Machholz 1 passed through the field of view of the C3 coronagraph. Several sequences of images were obtained at different positions of the filter and polarizer wheels. Four sets of them were suitable for further processing and only two sets could be used to determine the degree of polarization. There is also a long set of images taken with clear glass filter and short exposure where the comet is not oversaturated. The part of the comet orbit covered by the C3 coronagraph is shown in Fig. 2. Although the projection of the cometary orbit in the plane of vision appears to be very close to the Sun, the comet is not a sungrazer. Its highly inclined ($i = 60.18°$) orbit has a perihelion distance $q = 0.1241$ AU, and an eccentricity $e = 0.96$. The orbital period

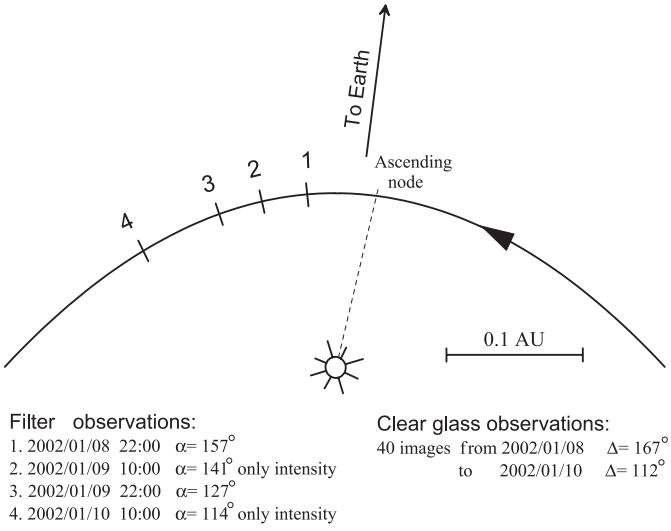


**Fig. 2.** Comet 69P/Machholz1 orbit near perihelion in 2002.

is 5.34 years. The comet went through perihelion on January 8, 15 UT. During the period of useful observations from Jan. 8, 08 UT to Jan. 10, 11 UT the phase angle a of the comet decreased from 167° to 114° and the heliocentric distance increased from 0.124 to 0.155 AU.

For the polarization measurements we also used C3 images of the comet from its apparition in October 1996. At that time the maximum phase angle was 113°. As at that time the corresponding polarizing filter was not yet damaged we had an opportunity to test the 0° image reconstruction procedure.

The position of the comet at the time of the exposures is shown in Fig. 2.

### 2.3. Data reduction

We had so-called Level 0.5 images at our disposal. This is raw data with brightness expressed as CCD detector counts. The database is available at `http://ares.nrl.navy.mil/database.html`. Figure 3 shows three representative images. Following the steps

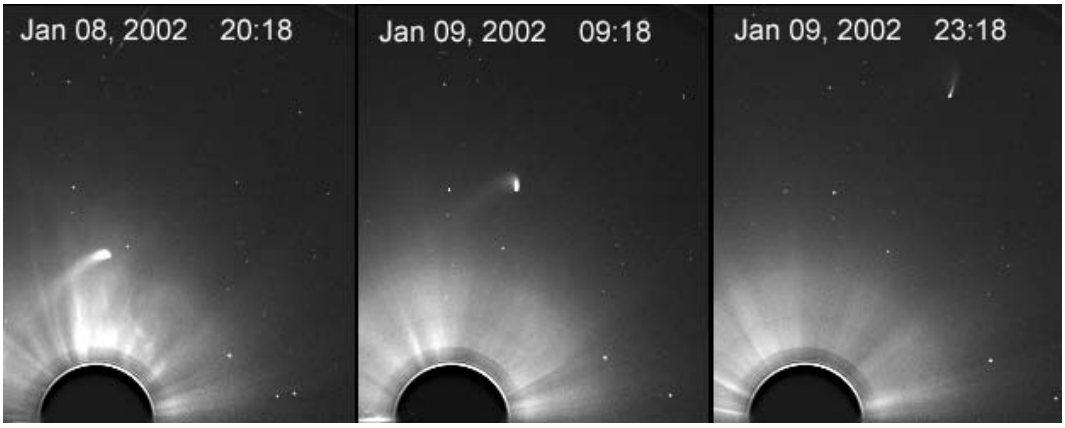


**Fig. 3.** LASCO C3 images of 96P/Machholz 1 near perihelion.

realized in the data reduction routines of the LASCO IDL library we subtracted the bias value, corrected for vignetting, and multiplied with the calibration factors (different for different color filters) to translate the data into physical units (mean solar disk brightness). No flatfields were applied to the data. Unfortunately no information about the level of instrumental polarization is available. Thus we do not make such a correction in our analysis, which in principle can give noticeable errors.

On those images where the comet is close to the Sun the bright solar corona is superimposed on the image of the comet. The irradiance of the corona could affect the result of the measurements. In a first step the influence of background was reduced by subtracting two images taken close in time. As the comet moves in the field, if the corona does not change between the two exposures the background would be fully eliminated in this step. To take into account possible changes of the corona between the two exposures, in a second step we marked an area around the comet and constructed an artificial background in this area by means of radial interpolation between the outer and inner sides of the marked area. We decided on radial interpolation because the structures of the solar corona are oriented mainly radially. This artificial background was then subtracted from the image. The remaining unevenness of the background field was of the order of 1% of maximum cometary brightness. Then, in the third step, the comet photometric center (maximum brightness in the cometary image) was searched in each frame and the values of the integrated flux were extracted within a square window of 3×3 pixels (168×168 arcsec) centered on the photometric center. We made one measurement of the flux from the comet and 5 additional measurements of background flux close to the comet. Then we calculated the average value for the background and subtracted it from the comet count. In this way the background subtraction was further improved and, from the standard deviation of the 5 measurements, an estimate of the error in the background determination was obtained. The resulting fluxes are plotted in mean solar flux units in Fig. 5. The errors connected with the uncertainty of the background are smaller than the plotting symbols. The main error shown in Figs. 5–7 is caused by the statistical uncertainty of the CCD detector counts. For each data point this error is equal to the square root of the corresponding number of counts multiplied by the CCD quantization step (i.e. the number of electrons per count) expressed in mean solar flux units. We note, however, that the absence of a useful flat field may cause systematic errors.

Up to here the described data reduction applies to photometry as well as polarimetry. Two additional steps were taken to obtain polarization values.

A synthesized image $I_{0^\circ}$ was calculated with the following formula:

$$I_{0^\circ} = 3 \cdot K \cdot I_{\rm clear} - I_{-60^\circ} - I_{+60^\circ}, \quad (1)$$

where $K$ is the factor connected with the absorption of light by the polarizing filter ($K = 0.2526$), $I_{\rm clear}$ is the clear image, and $I_{-60^\circ}$ and $I_{+60^\circ}$ are the images at the corresponding positions of the polarizer wheel.

After calculation of $I_{0^\circ}$ we had 3 measurements of brightness $I_{-60^\circ}$, $I_{0^\circ}$ , $I_{+60^\circ}$ at 3 polarizer positions. Then the linear polarization $P$ was deduced by applying the following formula:

$$P = 2\ [I_{-60^\circ}(I_{-60^\circ} - I_{0^\circ}) + I_{0^\circ}(I_{0^\circ} - I_{+60^\circ}) + I_{+60^\circ}(I_{+60^\circ} - I_{-60^\circ})]^{1/2} / \ (I_{-60^\circ} + I_{0^\circ} + I_{+60^\circ}). \quad (2)$$

In order to test the accuracy of the synthesis procedure one can compare $I_{0^\circ}$ values measured in 1996 with the ones derived from clear images. We found that the difference in the counts is within the limits of the measurement errors.

## 3. Results and discussion

### 3.1. Contribution of gas and plasma to our images

In this paper we are interested in the optical properties of cometary dust. However, the LASCO C3 filters transmit emissions of cometary gas and plasma as well. Therefore, before we draw conclusions on the optical properties of cometary dust we must discuss the possible presence of cometary gas and plasma. A faint plasma tail is clearly visible on the images taken shortly after minimum elongation of the comet from the Sun where it forms a large angle with the dust tail. Later in the observations the plasma tail merges into the dust tail and therefore

cannot be clearly recognized. Close to the cometary nucleus the plasma intensity is nearly constant while the dust intensity is strongly peaked (Bonev & Jockers 1994). Therefore close to the nucleus the plasma contribution can safely be neglected. The radiative lifetimes of the neutral coma molecules scale with the square of the heliocentric distance, i.e. at 0.15 AU the scale length of the $C_2$ coma, $\approx 10^5$ km at 1 AU, is reduced to 3000 km, i.e. the gas coma size is ≈6000 km, much less than the size of 1 pixel of the C3 camera, which amounts to 56 arcsec, i.e. about 40 000 km at the geocentric distance of the comet. As the cometary molecules emit fluorescence radiation their scattered radiation is isotropic while the dust scattering is expected to be peaked in the forward scattering direction. Therefore the relative contribution of radiation of the molecules will increase at smaller phase angles. As the very small size of the gas coma fills only a very small fraction of one pixel the measured brightness is most likely dominated by the scattered light from cometary dust.

### 3.2. Polarization

In Fig. 4 the results of the polarization measurements for three different filters at two apparitions (1996 and 2002) are presented. The error bars in these measurements are mostly due to the uncertainty in the background determination. The solid line represents a trigonometric fit to standard cometary polarimetric data. The curve is computed using the following analytic function:

$$P(\alpha) = b(\sin\alpha)^{c_1}(\cos(\alpha/2))^{c_2}\sin(\alpha - \alpha_0), \quad (3)$$

where the free coefficients $b = 31.72$, $c_1 = 0.815$, $c_2 = 0.408$ and the inversion angle $\alpha_0 = 21.2°$ are chosen for a typical dusty comet and the red continuum filter RC centered at 684 nm (Kiselev, private communication; for the curve see Kiselev & Velichko 1998) . As one can see, the accuracy of the polarization measurements is unsatisfactory, which makes further interpretation difficult. In general the measured values follow the standard curve of dust-rich comets, but the orange filter points from 1996, which actually should be of better quality as all three polaroids were functional at that time, deviate noticeably from this trend.

### 3.3. Phase function of intensity

The cometary brightness depends on heliocentric distance and on phase angle. Gehrz & Ney (1992) have presented albedo values A of comets derived from a comparison of observations in the visual and thermal infrared wavelength ranges. As the phase dependence of the thermal emission of cometary dust grains is expected to be small, the thermal emission of cometary dust is a measure of the dust production and $f(\alpha) = f_{\rm vis}/f_{\rm IR} = A/(1-A)$ is proportional to the phase dependence of the brightness. There are no brightness measurements of comet 96P/Machholz 1 in the thermal infrared during the time of the SOHO observations. Fortunately, during these observations the heliocentric distance changed very little (from 0.124 to 0.155 AU). To correct for the small changes in heliocentric distance we have used observations of comet Machholz 1 from

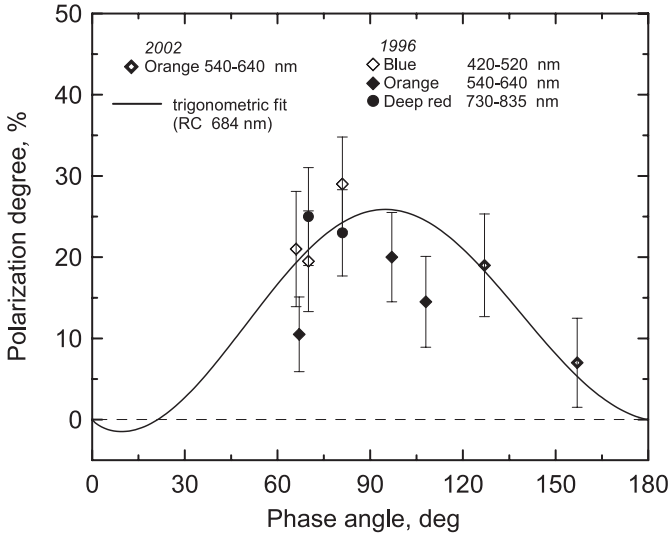


**Fig. 4.** Polarization observations with different color filters vs. phase angle. The solid curve is a trigonometric fit to the typical cometary dust polarization phase dependence observed at 684 nm.

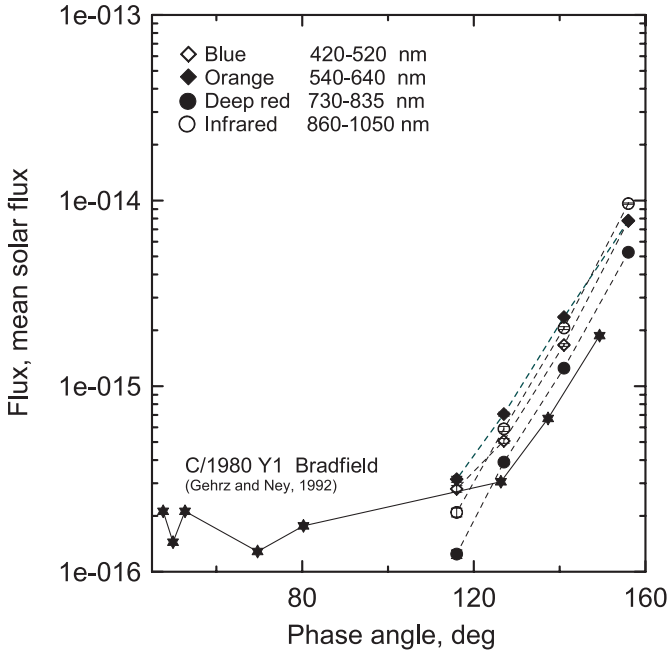


**Fig. 5.** Phase curves for comets 69P/Machholz 1 (circles and diamonds) for corresponding color filters and Bradfield 1980 XV (black stars). The values of comet Bradfield have been adjusted by multiplication with a constant to fit the measurements of comet Machholz 1.

1986 (Sekanina 1990) and extrapolated Eq. (1) of Sekanina's paper, describing the brightness variation of the comet with heliocentric distance, to our near-perihelion case. Note that at the phase angles where the photometric measurements quoted by Sekanina were taken the phase dependence can be neglected. Normalizing Eq. (1) of Sekanina (1990) to 1 at perihelion passage, at the largest heliocentric distance of our data of 0.155 AU we get a correction of the observed brightness by a factor of 1.30. Compared to the large brightness gradient in our data the correction is almost negligible.

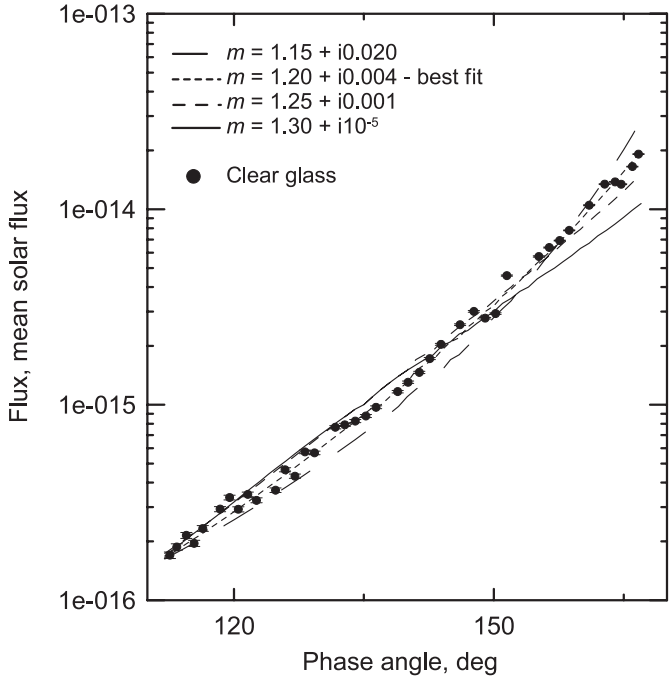


**Fig. 6.** Theoretical best fit curves for the clear glass measurements at four combinations of $n$ and $k$.

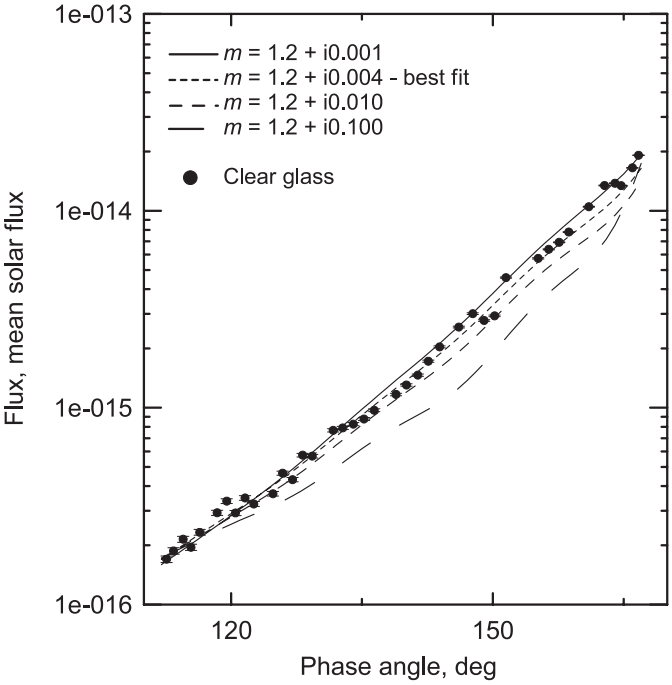


**Fig. 7.** Dependence of the phase function on the absorption index at $n = 1.2$.

In Fig. 5 the resulting phase dependence of the flux of 96P/Machholz 1, with the dependence on heliocentric distance reduced to perihelion, is shown in mean solar flux units for the different wavelength bands and for the clear glass filter. They are calculated from the nominal calibrations of the C3 coronagraph and may not be sufficiently accurate to allow the determination of reddening (i.e. the increase of brightness with wavelength). In what follows we will only make use of the gradient of brightness with respect to phase angle. The curves are compared with a measurement of comet C/1980 Y1 (Bradfield) (Gehrz & Ney 1992), which is the only other comet known to us which was observed at phase angles larger than 120°. The quantity $f_{\rm vis}/f_{\rm IR}$ given in Gehrz & Ney (1992) was multiplied with an arbitrary scale factor to produce a curve close to our measurements of comet 96P. All the curves show a steep decrease of total brightness with decreasing phase angle.

Cometary dust particles have irregular shapes and, probably, complex structures. So one should apply a proper light scattering model, which takes into account the complex structure of the particles. In the forward scattering part of the phase curve the light scattering of particles comparable to the wavelength is dominated by diffraction. However, we do not see any evidence for the diffraction spike in the obtained phase curves. The absence of a diffraction spike can be used to obtain a lower limit for the size of the particles, as for particles having a size parameter $x = 2\pi r/\lambda$ (where $r$ is radius of the particle and $\lambda$ is the wavelength) larger than ≈20 the first forward scattering diffraction minimum is already ≤167°, i.e. beyond the range of the observed phase angles. We can therefore conclude that the particles predominantly contributing to the observed scattered radiation must have a size parameter larger than $x \approx 20$, i.e. have a radius larger than 1 $\mu$m. Phase curves of particles of sizes larger than 1 $\mu$m have been measured by Weiss-Wrana (1983) and Volten et al. (2001). Calculations have been performed by Macke et al. (1995), by Grundy et al. (2000) and more recently by Grynko & Shkuratov (2003). Up to now large particles can only be studied with the T-matrix method and the geometric optics approximation. The first method is more accurate but applicable only to rotationally symmetric particles. The second is more approximate but can be used for arbitrary sizes and shapes. For particles where both methods can be applied the results agree for size parameters $x \geq 30$–60 (Macke et al. 1995). The phase curves produced by these authors show a very narrow diffraction spike at small scattering angles which for particles of size parameter $x = 30$ ends at about 10° scattering angle. For larger scattering angles the decrease of the phase curve is linear, in agreement with our observations. Calculations using the geometric optics approximation are independent of particle size if the particles are nonabsorbing. The gradient of the phase curves of such particles strongly increases with decreasing real part of the refractive index. A similar but weaker dependence exists for rising imaginary part of the refractive index (Grundy et al. 2000; Grynko & Shkuratov 2003). According to Grynko & Shkuratov (2003), compared to the backscattering part, the forward scattering part of the phase function is much less dependent on particle shape. This is because the forward scattering slope, at least for the larger particle sizes, is formed mostly by rays transmitted by the particle without any further interaction. Therefore in this phase angle domain phase functions for spheres and irregular particles behave in a similar way (see also Weiss-Wrana 1983). Thus we can apply Mie theory to extract the complex refractive index $m = n + ik$ from the measured brightness gradient.

Presently the size distribution of dust grains in comets is a matter of debate (see e.g. Jockers 1997). Space observations of Halley's comet (Mazets et al. 1986) have revealed particle size

distributions of the particle fluences $dn = r^{-a}\,dr$, where $dn$ is the number of dust grains in a small interval around radius $r$, and $a$ is the power index. For the small submicron particles the space observations indicate power indices $a \approx 2$ which increase to $\approx 3$ and more with increasing size. But for the large particles of interest here the statistics are poor and, worse, because of the high encounter speed at comet Halley no good calibrations of the measuring device were available. Also it is not clear if comet Halley is representative for all comets or at least for comet Machholz 1. Additional information comes from models (mostly by Fulle and coworkers) of dust tails of a number of comets based on the radiation pressure force. Power indices of dust production are provided in Table II of Jockers (1997). In a more recent paper (Fulle et al. 2000) the particle data as well as the optical data on comet Halley obtained by the Giotto probe are combined into a similar radiation pressure model and a power index of 2.7 is derived. Because we are interested here in fluences along the line of sight we must correct the power indices of dust production for the fact that smaller particles have larger emission speeds. After correction these power indices are lowered by a number between 0 and 0.5, i.e. become significantly less than 3.

Using Mie theory we have performed calculations of the phase functions for $a = 2.5$. In our calculations we restricted the range of size parameter $x$ between 10 and 400, since the presence of smaller and larger particles influences the result very little. The number of large particles decreases according to the distribution law. On the other hand, small particles do not have a high enough scattering efficiency to make a significant contribution to the phase function behavior at $a = 2.5$. Besides, they introduce a noticeable wavelength dependence of the scattering, which is absent in our data (see Fig. 5).

In order to determine the real and imaginary part of the refractive index $m = n + ik$ we proceeded as follows. For four fixed values of $n$ we determined the best fit absorption indices $k$. In Fig. 6 one can see that the best fit refractive indices $m$ produce gradients close to the observed phase curve (clear glass filter). Higher refraction is coupled with lower absorption and vice versa. The best coincidence corresponds to $m = 1.2 + i\,0.004$. Higher and lower values of $n$ give certain deviations from the measurements at all $k$. Then we tried to find the maximum possible $k$ at $n = 1.2$. Fig. 7 shows that the increase of the absorption index in the very wide range from $k = 0.001$ to 0.1 leads to small changes in the phase dependence, keeping the same gradient in the given limits of the phase angles.

Simple application of Mie theory gives unrealistically low values for the refractive index. As all conceivable constituent minerals of cometary dust have higher refractive indices we assume that the particles are not single homogeneous grains, but porous aggregates of smaller grains. The calculated values of the complex refractive index are considered as an "effective" refractive index $m_{\rm eff} = n_{\rm eff} + i\,k_{\rm eff}$ in terms of effective medium theory and the porosity $P$ is introduced as an additional free parameter. The case of grains composed of a single porous material can be treated with the Maxwell-Garnett (Bohren & Huffman 1983) and Bruggeman (Bruggeman 1935) formulae taking vacuum ($m = 1$) as the "host" material and filled subvolumes as the "inclusion". Both formulae provide practically equal results. For example, a porosity rate $P = 0.5$ changes the value of the complex refractive index from $m = 1.2 + i\,0.004$ to $m = 1.43 + i\,0.009$.

Corrigan et al. (1997) found that interplanetary dust particles, which can perhaps serve as examples for cometary particles, have a porosity which very rarely exceeds $P = 0.3$. The maximum real part of the complex refractive index that we can obtain with $P \leq 0.5$ using a mixing rule is around $n = 1.65$, but in this case the particles must be very transparent. In order to fit the data using higher absorption of the dust particles one must assume either a higher porosity rate, which seems to be unlikely, or an unrealistically low real part of the refractive index.

Water ice has a refractive index $n$ of $\approx 1.3$ and therefore may seem well suited to explain the refractive index derived in our models. Water ice has been detected by the ISO spacecraft in comet C/1995 O1 (Hale-Bopp) at heliocentric distances $r \geq 2.9$ AU by Lellouch et al. (1998) but is very unlikely to be present at $r \leq 0.16$ AU (Hanner 1981).

## 4. Conclusions

From measurements of brightness and polarization of comet 96P/Machholz 1 photographed with the SOHO-LASCO C3 coronagraph at phase angles up to 167° and 157° , respectively, we found the following:

The accuracy of the polarization measurements proved to be low. In general the polarization data follow the phase law $P(\alpha) = 31.72\sin(\alpha)^{0.815}\cos(\alpha/2)^{0.408}\sin(\alpha - 21.2°)$ characteristic of a typical dusty comet.

The brightness increases linearly by almost two orders of magnitude in the given range of phase angles. The gradient is independent of wavelength.

The forward scattering diffraction spike is absent on the phase curve. Therefore we conclude that the contributing grains must have a size parameter larger than $x \approx 20$, i.e. have a radius larger than 1 $\mu$m. The best fit refractive index of the data is $m = 1.2 + i\,0.004$ according to Mie calculations of particles having a power law distribution of power index $\approx 2.5$. On the assumption of a particle porosity $P = 0.5$ application of the mixing rules gives a complex refractive index of particles $m = 1.43 + i\,0.009$. At lower porosity particles must either be very transparent or have an unrealistically low real part of the refractive index.

*Acknowledgements.* We thank the whole LASCO team for making the data used here available to us and in particular Dr. Doug Biesecker for providing the required explanations.
The German effort for SOHO has been supported by the DLR (Deutsches Zentrum für Luft- und Raumfahrt e.V. in Bonn). SOHO is a mission of international cooperation between ESA and NASA.

## References

Bohren, C. F., & Huffman, D. R. 1983, Absorption and Scattering of Light by Small Particles (New York: John Wiley)
Bonev, T., & Jockers, K. 1994, Icarus, 107, 335

Brueckner, G. E., Howard, R. A., Koomen, M. J., et al. 1995, Sol. Phys., 162, 357
Bruggeman, D. 1935, Annalen der Physik, 24, 636
Corrigan, C. M., Zolensky, M. E., Dahl, J. et al. 1997, Meteoritics & Planet. Sci., 32, 509
Fulle, M., Levasseur-Regourd, A. C., McBride, N., & Hadamcik, E. 2000, AJ, 119, 1968
Gehrz, R., & Ney, E. 1992, Icarus, 100, 162
Grundy, W. M., Doute, S., & Schmitt, B. 2000, J. Geophys. Res., 105, 291
Grynko, Ye., & Shkuratov, Yu. 2003, JQSRT, 78, 319
Hanner, M. S. 1981, Icarus, 47, 342
Hadamcik, E., & Levasseur-Regourd A.-C. 2003, Icarus, 166, 188
Jockers, K. 1997, Earth, Moon and Planets, 79, 221
Kiselev, N., & Velichko, F. 1997, Earth, Moon and Planets, 78, 347
Kiselev, N., & Velichko, F. 1998, Icarus, 133, 286
Kiselev, N., Jockers, K., & Rosenbush, V. 2002, Earth, Moon and Planets, 90, 167
Lellouch E., Crovisier J., Lim, T., et al. 1998, A&A, 339, L9
Macke, A., Mishchenko, M. I., Muinonen, K., & Carlson, B. E. 1995, Opt. Lett., 20, 1934
Mazets, E.P., Aptekar, R.L., Golenetskii, S. V., et al. 1986, Nature, 321, 276
Sekanina, S. 1990, AJ, 99, 1268
Volten, H., Muñoz, O., Rol, E., de Haan, J. F., & Hovenier, J. W. 2001, J. Geophys. Res., 106, 375
Weiss-Wrana, K. 1983, A&A, 126, 240